

# Image Corruption-Inspired Membership Inference Attacks against Large Vision-Language Models

Zongyu Wu, Minhua Lin, Zhiwei Zhang, Fali Wang, Xianren Zhang,  
Xiang Zhang, Suhang Wang

The Pennsylvania State University

{zongyuwu, mfl15681, zbz5349, fqw5095, xzz5508, xzz89, szw494}@psu.edu

## Abstract

Large vision-language models (LVLMs) have demonstrated outstanding performance in many downstream tasks. However, LVLMs are trained on large-scale datasets, which can pose privacy risks if training images contain sensitive information. Therefore, it is important to detect whether an image is used to train the LVLM. Recent studies have investigated membership inference attacks (MIAs) against LVLMs, including detecting image-text pairs and single-modality content. In this work, we focus on detecting whether a target image is used to train the target LVLM. We design simple yet effective **Image Corruption-Inspired Membership Inference Attacks (ICIMIA)** against LVLMs, which are inspired by LVLM’s different sensitivity to image corruption for member and non-member images. We first perform an MIA method under the white-box setting, where we can obtain the embeddings of the image through the vision part of the target LVLM. The attacks are based on the embedding similarity between the image and its corrupted version. We further explore a more practical scenario where we have no knowledge about target LVLMs and we can only query the target LVLMs with an image and a question. We then conduct the attack by utilizing the output text embeddings’ similarity. Experiments on existing datasets validate the effectiveness of our proposed attack methods under those two different settings.

## 1 Introduction

Large Vision-Language Models (LVLMs) (Liu et al., 2024a,b; Bai et al., 2023b; Achiam et al., 2023), which can generate text outputs based on visual and/or textual input, are attracting increasing attention. Many LVLMs have been developed, which have shown great performance on various tasks (Dong et al., 2024; Xu et al., 2024; Wu et al., 2025; Yue et al., 2024; Li et al., 2024a; Bucciarelli

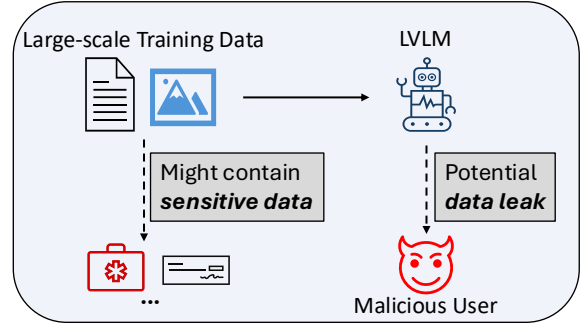


Figure 1: An example of some potential risks in LVLMs.

et al., 2024) such as biomedical question answering (Li et al., 2023a).

Despite their great success, LVLMs have also raised critical concerns about privacy and copyright issues as shown in Figure 1. LVLMs are usually trained on large-scale datasets (Ng et al., 2020; Changpinyo et al., 2021; Byeon et al., 2022). The training data might contain sensitive information, such as unauthorized medical data and copyrighted content. Previous works have shown that neural networks, especially large models, can memorize training data (Song et al., 2017; Carlini et al., 2019, 2022b). Thus, the memorization phenomena might also happen in LVLMs and inadvertently cause training data leakage (Li et al., 2024b), which could cause substantial loss to data owners. Hence, knowing whether one’s data is used to train an LVLM is important for privacy and copyright protection.

Membership inference attacks (MIAs), which aim to determine whether a given sample is used to train a model (Hu et al., 2022a; Shokri et al., 2017), are critical for ensuring data integrity (Oren et al., 2023; Duan et al., 2024). Generally, models tend to overfit to the training data, resulting in higher prediction confidence for member data (data used for training) than non-member data. Many traditional MIA methods adopt such nuance difference in model prediction to differentiate members and

non-members.

Recently, some works (Ko et al., 2023; Li et al., 2024b; Hu et al., 2025) have explored the MIA on vision-language models, from CLIP (Radford et al., 2021) to LVLMs (Zhang et al., 2023). Ko et al. (2023) focus on determining whether an image-text pair exists in the training data of CLIP. However, detecting whether an image in the training data is more practical than detecting the entire image-text pair as the image owner might only have the image without text while the text description might be labeled by the model trainer (Li et al., 2024b).

Therefore, we study the problem of single-image based MIA against LVLMs. The work in this direction is rather limited (Li et al., 2024b). Li et al. (2024b) also conduct MIA on a single modality (Image or textual description) against LVLMs by using the output logits of LVLM. Instead of using output logits, we propose a new perspective, i.e., adopting image embedding from the visual part of LVLMs. Our intuition is: as the model has seen member images, it should be able to give robust image embedding of a member image even if some details of the image are missing. In other words, *the image embedding of a member is more robust to image corruption than that of non-member images*, which is verified by our preliminary experiment in Section 3 (see Fig. 3). Based on this observation, we propose a novel MIA algorithm under the white-box setting, where we can obtain the image embedding from LVLMs. Given an image, we corrupt the image and utilize the image embedding similarity between the raw image and the corrupted version to determine if an image is a member. A higher similarity means the image is more likely to be a member.

However, for many closed-source LVLMs, we cannot obtain image embeddings. To address this issue, we extend the similarity to the output text level. Our assumption is: robust image embedding of member image will result in robust text generation under perturbation, which is also verified in Figure 4. Based on this observation, we extend our framework to black-box setting, where we can only obtain output texts from LVLMs. Given a target image, we corrupt the image and compare the generated text similarity between the raw image and its corrupted version. A larger text similarity means the image is more likely to be a member.

Our **main contributions** are: (i) In this work, we investigate two membership inference attack scenarios targeting LVLMs. For each setting, we

propose one simple yet strong attack method that leverages the model’s robustness to image corruption on its training images; (ii) Extensive experiments on existing datasets show the effectiveness of the proposed method.

## 2 Related Works

### 2.1 Large Vision-Language Models

Large Vision-Language Models (Bai et al., 2025; Chen et al., 2024a,b; Liu et al., 2024b,a; Chen et al., 2024c; Tong et al., 2024; Zhu et al., 2025; Young et al., 2024; Zhu et al., 2023; Chen et al., 2023; Li et al., 2024c; Du et al., 2025), also known as multimodal large language models (Fu et al., 2024) are developing rapidly due to the success of language models (Wang et al., 2024; Zhao et al., 2023; Chiang et al., 2023; Touvron et al., 2023a,b; Grattafiori et al., 2024; Yang et al., 2025, 2024; Jiang et al., 2023; Team, 2023; Penedo et al., 2023) such as Qwen (Bai et al., 2023a; Yang et al., 2024) and LLaMA series (Touvron et al., 2023a,b). These models, like LLaVA 1.5 (Liu et al., 2024c), can generate textual outputs given textual questions and images.

### 2.2 Membership Inference Attack

Membership Inference Attack (MIA) (Shokri et al., 2017; Salem et al., 2018; Sablayrolles et al., 2019; Li et al., 2021; Hu et al., 2022a; Nasr et al., 2019; Leino and Fredrikson, 2020; Rezaei and Liu, 2021) tries to determine whether a given data sample was used to train a machine learning model (Shokri et al., 2017).

One main category of MIA methods is metric-based (Hu et al., 2022a; Li et al., 2024b; Sablayrolles et al., 2019; Choquette-Choo et al., 2021; Li et al., 2021), which use some well-designed metrics, such as the entropy of output logits, to determine the membership status of a given sample. Another main category is methods based on shadow training (Shokri et al., 2017), which trains some shadow models to simulate the target model and then conducts MIAs based on these shadow models. Many later works have started to explore the MIA on LLMs (Mattern et al., 2023; Mireshghalah et al., 2022; Ren et al., 2024; Shi et al., 2024; Zhang et al., 2024) such as Min-K% (Shi et al., 2024) and Min-K%++ (Zhang et al., 2024).

With the development of multimodal learning, there are also some works exploring MIA on multimodal models (Hu et al., 2022b; Ko et al., 2023;

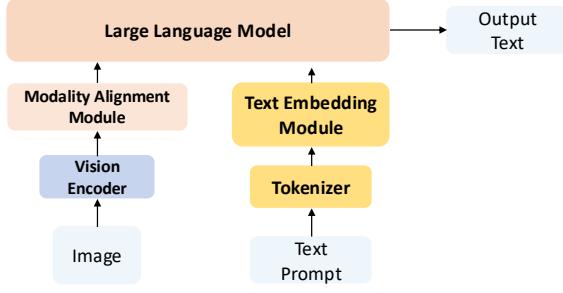


Figure 2: An illustration of the architecture of large vision-language models (Liu et al., 2024a).

Li et al., 2024b). We focus on vision-text here. Liu et al. (2021) studies MIAs on image encoder models such as CLIP vision encoder (Radford et al., 2021). It calculates the similarity scores between the augmented images’ embeddings and the scores are then used to train a classifier to infer the member status of an image. Ko et al. (2023) work on detecting whether an image-text pair is in the training data of CLIP models (Radford et al., 2021). Li et al. (2024b) investigates the single-modality MIA in LVLMs, which is a more practical scenario. They calculate the Rényi Entropy (Rényi, 1961) based on different slices of logits. Hu et al. (2025) found that member data and non-member data have different sensitivity to temperature. They then perform four attack methods under four different settings to detect whether a group of images is used in the training stage.

Our work is inherently different from existing work: We propose a new perspective from image embedding robustness and output text robustness of the member image under image corruption, which works for both white-box and black-box settings.

### 3 Preliminaries

In this section, we give the necessary background information and formulate the problems.

#### 3.1 Large Vision-Language Models

As shown in Fig. 2, an LVLM  $M_\theta$  usually consists of three parts: A vision encoder  $f_{Vision}$ , an LLM  $f_{LLM}$ , and a modality connection module  $f_{Align}$ . The vision encoder  $f_{Vision}$ , e.g., CLIP (Radford et al., 2021), takes an image  $x$  as input and outputs the embeddings of  $N$  image patches  $\{z_1, \dots, z_N\}$ , where  $z_i \in \mathbb{R}^{d_v}$  is the  $i$ -th patch embedding with  $d_v$  being the embedding dimension. The patch embeddings are then transformed into an embedding sequence  $\mathbf{E}^v = \{e_1^v, \dots, e_N^v\}$  which is in the em-

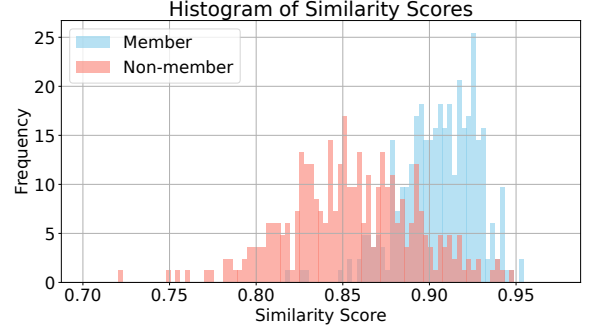


Figure 3: A histogram of similarity scores of corrupted images’ (Through Gaussian Blur) embeddings and original images’ embeddings for member and non-member data. Scores in this figure achieve an AUC of 0.881.

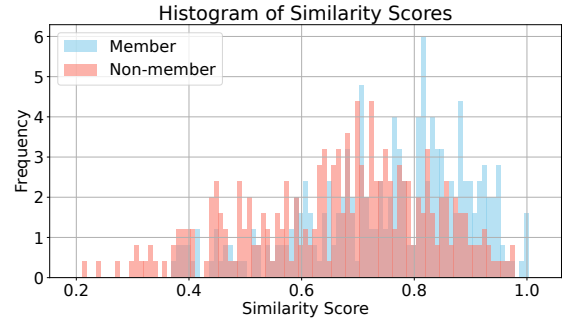


Figure 4: A histogram of similarity scores of textual output embeddings between corrupted images (Through Gaussian Blur) and the original images for member and non-member data. Scores in this figure achieve an AUC of 0.652.

bedding space of  $f_{LLM}$  using  $f_{Align}$ . Each element in  $\mathbf{E}^v$  can be represented as:

$$e_i^v = f_{Align}(z_i), \quad (1)$$

The text prompt  $T_{in}$ , composed of the instruction and the question, is encoded into an embedding sequence of tokens  $\mathbf{E}^t = \{e_1^t, \dots, e_K^t\}$ , where  $K$  is the number of tokens. Finally, the text embedding and the image embeddings are used as input to the LLM  $f_{LLM}$  to get the text output as  $T_{out} = f_{LLM}(\mathbf{E}^v, \mathbf{E}^t)$ .

#### 3.2 Threat Model

**Attacker’s Goal.** Given a trained LVLM  $M_\theta$ , the attacker’s goal is to determine if a specific image was in the training set of the target LVLM  $M_\theta$ . The attackers only have the target image and do not require its corresponding ground-truth text description. The problem is formally defined as:

**Definition 1 (Image Only MIA)** Given a trained LVLM  $M_\theta$  and a target image  $x_t$ , the attacker aims

to determine whether  $\mathbf{x}_t$  was part of the training data for  $\mathbf{M}_\theta$ , i.e.,  $\text{Attack}(\mathbf{M}_\theta, \mathbf{x}_t, T_{in}) \rightarrow \{0, 1\}$ , where  $T_{in}$  is the input textual instruction.  $\mathbf{x}_t$  is considered to be in the training set (i.e., member image) if the output is 1. Otherwise,  $\mathbf{x}_t$  is a non-member.

**Attacker’s Knowledge.** In our work, we consider two practical settings, i.e., white-box and black-box. (i) **White-box Setting.** In this setting, the attacker can get the embedding of the image, i.e., the embedding through the model’s vision encoder and modality alignment module. This is practical for open-source LVLMS. (ii) **Black-box Setting.** In this setting, the attacker can only query the LVLMS  $\mathbf{M}_\theta$  with image input  $\mathbf{x}$  and text input  $T_{in}$  to get the text output  $T_{out}$ . The attacker has no knowledge of the target model. This setting is more realistic for commercial LVLMS.

### 3.3 Intuition for Performing MIA

As we are only given the image, how to fully utilize the image to determine if the image remains a challenging question. Inspired by Liu et al. (2021) that a CLIP vision encoder tends to overfit to its training data and member images show higher similarity for two augmented versions, we assume that **the image embedding of a member image from the vision encoder and modality alignment module should be more robust to image corruption than that of non-member images**. The intuition is, if the model has seen the image and memorized the image, then even if the image is corrupted, e.g., some details missing, the model can still recall the details and result in embedding similar to the original one. To verify our assumption, for each image, we first apply *Gaussian Blur* (Bratski, 2000) as the corruption method to obtain the corrupted image, where Gaussian Blur is a smoothing technique that reduces image detail and noise by averaging pixels with a weighted Gaussian kernel. We compute the similarity score between the embedding of the original image and that of its corrupted version. The chosen model is LLaVA-1.5-7B (Liu et al., 2024a), and the dataset is the Img\_Flickr dataset constructed by Li et al. (2024b). The similarity scores of member images and non-member images are shown in Figure 3. We can observe that member images normally show a higher similarity score than non-member images, which aligns well with our assumption. The scores show a clear difference between the two groups, which suggests that the

similarity score between the original image embedding and its corrupted version’s embedding can be used to perform an image membership inference attack. Thus, we can utilize the robustness of member image embedding to determine its membership.

However, in black-box setting, we are unable to obtain the image embedding. As image embedding of member image is robust, it might also result in robust text even if the image is corrupted. Thus, we assume that **given the same text prompt (Instruction), an image seen during the LVLMS’s training process will produce a text output that is more similar to the output generated from its corrupted version, compared to images not included in the training data**. To verify our assumption, we use the same dataset, model, and corruption method as above. We compute the similarity score between the output text embeddings of the original and corrupted versions of each image, given the same prompt, separately. The results are shown in Figure 4. We observe that the discrepancy in similarity between member and non-member images still exists and can serve as a metric, although it is less apparent in Figure 3.

## 4 Method

Based on observations that LVLMSs are more robust to corruptions on members than non-members, we propose a novel framework, ICIMIA (Image Corruption-Inspired Membership Inference Attacks against Large Vision-Language Models). As shown in Figure 5, our method first produces a corrupted version  $\mathbf{x}'_t$  for the target image  $\mathbf{x}_t$ . Then both the  $\mathbf{x}_t$  and  $\mathbf{x}'_t$  are utilized to get their image embeddings or corresponding output text embeddings. Finally, we calculate the image/text embedding similarity as a metric. The image is viewed as a member image if the similarity score is bigger than a certain threshold. Next, we introduce the details.

### 4.1 White-Box MIA via Image Similarity

We first discuss the grey-box setting where we can obtain the embeddings of a given image through the vision encoder and modality alignment module.

Based on our observation in Section 3.3, the embeddings of trained images should be more robust to image corruption methods. To be specific, compared to images not used during training (Non-member data), the embeddings of the corrupted image and its original counterpart are normally more



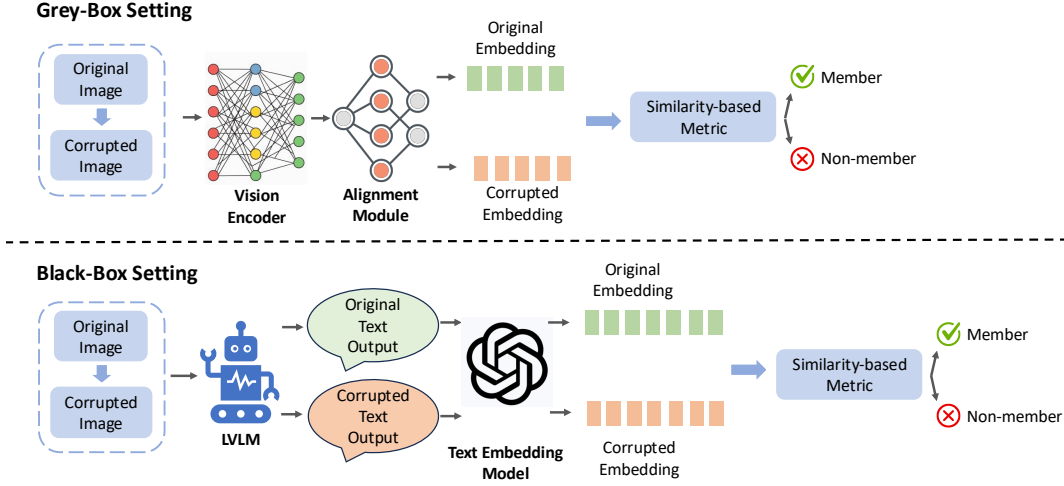


Figure 5: An illustration of the attack pipeline under two different settings.

---

**Algorithm 1** Image Similarity-based MIA

---

**Input:** Target image  $\mathbf{x}_t$ , threshold  $\lambda$

**Output:** Membership Prediction Result  $\in \{0, 1\}$

- 1: Obtain the embedding  $\mathbf{E}^v$  of  $\mathbf{x}_t$
  - 2: Apply corruption on  $\mathbf{x}_t$  to get image  $\mathbf{x}'_t$
  - 3: Obtain the embedding  $\mathbf{E}^{v'}$  of  $\mathbf{x}'_t$
  - 4: Compute similarity score  $s_{img}$  via Eq. 2
  - 5: **if**  $s_{img} < \lambda$  **then**
  - 6:      $\mathbf{x}_t$  is viewed as a non-member image
  - 7: **else**
  - 8:      $\mathbf{x}_t$  is viewed as a member image
  - 9: **end if**
- 

similar for images that were used in the training process (Member data). Therefore, we can use the similarity score as a metric to determine whether an image is used to train the LVLm.

The pipeline of our proposed framework is shown in the upper part of Figure 5. For a target image  $\mathbf{x}_t$  that we wanna detect, we first apply some corruptions to get a corrupted image as  $\mathbf{x}'_t = \text{Corruption}(\mathbf{x}_t)$ . Various corruption techniques can be used, such as Gaussian blur (Using a Gaussian Kernel). Then, we get the image embeddings for both the original image and the corrupted one. Last, we measure how close each patch embedding pair is and calculate the mean value as

$$s_{img} = \frac{1}{N} \sum_{i=1}^N \text{Sim}(\mathbf{e}_i^v, \mathbf{e}_i^{v'}) \quad (2)$$

where  $\mathbf{e}_i^v$  is the embedding of the  $i$ -patch of image  $\mathbf{x}_t$  obtained by Eq. 1 and  $\mathbf{e}_i^{v'}$  denotes the  $i$ -patch embedding of the corrupted image  $\mathbf{x}'_t$ .  $N$  is the

number of patches.  $\text{Sim}$  is a similarity function. We use cosine similarity here. The larger the  $s_{img}$  is, the more likely the image is viewed as a member image. The target image  $\mathbf{x}_t$  is predicted as a member image if  $s_{img}$  is bigger than a threshold  $\lambda$ .

Algorithm 1 summarizes the image similarity-based attack.

#### 4.2 Black-box MIA via Text Similarity

For many commercial LVLms, we are not able to obtain image embeddings. Thus, we study a more practical black-box setting where we know nothing about the target model but can only query the model with the target image and prompt to obtain the response text. Though we cannot obtain the image embedding, as the image embeddings of member images are robust to random corruption, correspondingly, the generated response text will be robust to the corruption, which is also verified in 3.3. This motivates us to query the target model using the original image and its corrupted version. Then we calculate pair-wise output text similarities.

Specifically, we feed the original target image  $\mathbf{x}_t$  and a text prompt  $T_{in}$  into the target LVLm and get an output  $T_{out}$  as  $T_{out} = f_{LVLm}(\mathbf{x}_t, T_{in})$ . Similarly, we get an output  $T'_{out}$  for the corrupted image  $\mathbf{x}'_t$  with the same input text prompt  $T_{in}$ . We then employ a text embedding model to get the embeddings of  $T_{out}$  and  $T'_{out}$ . With the text embedding, we calculate their similarity as

$$s_{text} = \text{Sim}(\text{Emb}(T_{out}), \text{Emb}(T'_{out})) \quad (3)$$

where  $\text{Emb}()$  denotes a text embedding model,

---

**Algorithm 2** Text Embedding Similarity-based Attack

---

**Input:** Target image  $x_t$ , Prompt  $T_{in}$ , threshold  $\lambda$

**Output:** Membership Prediction Result  $\in \{0, 1\}$

- 1: Feed the target LVLM with the target image  $x_t$  and a text prompt  $T_{in}$  and get output  $T_{out}$
  - 2: Apply corruption to get corrupted image  $x'_t$
  - 3: Feed the target LVLM with the corrupted target image  $x'_t$  and the same text prompt  $T_{in}$  and get output  $T'_{out}$
  - 4: Get the text output embedding  $Emb(T_{out})$  and  $Emb(T'_{out})$  of the original image and corrupted image
  - 5: Calculate the output similarity using Eq. 3
  - 6: **if**  $s_{text} < \lambda$  **then**
  - 7:      $x_t$  is viewed as a non-member image
  - 8: **else**
  - 9:      $x_t$  is viewed as a member image
  - 10: **end if**
- 

such as OpenAI’s text-embedding-3-small model<sup>1</sup>. Sim is a similarity function as in Eq. 2 which is a cosine similarity function. Similarly,  $x_t$  is considered member data if  $s_{text} > \lambda$ . This method is summarized in Algorithm 2.

In this section, we evaluate our methods on existing datasets to answer the following research questions: (i) How well do our proposed methods perform in conducting membership inference attacks against large vision-language models? and (ii) What are the impacts of hyperparameters?

### 4.3 Experimental Setup

**Evaluation Metric.** Following previous work (Li et al., 2024b), we use Area Under the Curve (AUC) and True Positive Rate at 5% False Positive Rate (TPR at 5% FPR) as the evaluation metrics. For both metrics, higher values indicate better MIA performance. The descriptions of these metrics can be found in Appendix C.

**Datasets** We test our method on two benchmark datasets, VL-MIA/Flickr and VL-MIA/Flickr-2k (Li et al., 2024b). The details of datasets can be found in Appendix A.

**Computational Resources.** We conduct all experiments on machines equipped with four NVIDIA RTX A6000 GPUs (48GB memory).

**Selected Models.** We evaluate our method on two models: LLaVA 1.5 7B, and LLaVA 1.5 13B (Liu

et al., 2024a). The models are chosen as they are classical and the datasets are applicable to them.

**Corruption Methods.** We choose the following corruption methods: (i) *Gaussian Blur*: This is a technique that makes image soft and blurry using a Gaussian Kernel; (ii) *Motion Blur*: We apply a custom convolution kernel, mimicking the effect of horizontal motion-blur; and (iii) *JPEG Compression*: This is a method to compress the image to get the corrupted version. We apply CV2 (Bradski, 2000) to achieve Gaussian Blur and Motion Blur. We put some examples of different corruption techniques in Appendix B.

**Baselines.** We adopt representative and state-of-the-art MIA methods against LVLMs, including: (i) **AugKL** (Li et al., 2024b; Liu et al., 2021): Li et al. (2024b) extend the approach designed by Liu et al. (2021) to LVLMs. Specifically, Li et al. (2024b) quantify the difference between the original and augmented images (Such as Crop and Rotation) by computing the KL divergence between their distributions of logits; (ii) **Max\_Prob\_Gap** (Li et al., 2024b): It is the average value of the difference between the highest and second-highest token probabilities at each position. (iii) **Min-K** (Shi et al., 2024): Min-K is an MIA method designed for LLMs. It uses a ground-truth token and computes the lowest K% of its predicted probabilities. Li et al. (2024b) extends it to the LVLM domain; (iv) **Perplexity**: It is based on loss. Li et al. (2024b) analyze target perplexity to achieve the attacks (Carlini et al., 2021); (v) **MaxRényi-K** (Li et al., 2024b): It selects the top K% tokens with the highest Rényi entropy. Then the value is the average value of these entropies; and (vi) **Mod-Rényi** (Li et al., 2024b): This is an extended version of MaxRényi-K which is designed for target-based scenarios.

## 5 Experiment

**Implementation details.** All these baselines need the knowledge of the target model’s tokenizer and the output logits. The implementations of all baselines are based on Li et al. (2024b). Following the recommendation of Shi et al. (2024) and Li et al. (2024b), we set  $K = 20$  for the Min-K method.  $K$  is set to 0, 10, and 100 for MaxRényi- $K\%$  and  $\alpha$  is chosen over 0.5, 1, and 2 for both ModRényi and MaxRényi- $K\%$ , as in Li et al. (2024b). We report the highest AUC for each method and provide the TPR at 5% FPR using the hyperparameter combination that achieves this highest AUC. For the

---

<sup>1</sup><https://platform.openai.com/docs/models/text-embedding-3-small>

Table 1: Image MIA AUC of various baseline methods under Li et al. (2024b)’s pipeline and our proposed approach on VL-MIA/Flickr. For all the baselines, the term "img" refers to the logits segment associated with the image embedding, while "inst" represents the instruction segment. "desp" corresponds to the generated description’s logits segment, and "inst+desp" denotes the combination of the instruction and description segments.

Method	LLaVA-1.5-7B				LLaVA-1.5-13B			
	img	inst	desp	inst+desp	img	inst	desp	inst+desp
Perplexity	-	0.378	0.665	0.558	-	0.440	0.707	0.646
Min_20% Prob	-	0.374	0.672	0.370	-	0.454	0.684	0.433
ModRényi	-	0.370	0.658	0.613	-	0.442	0.703	0.678
Max_Prob_Gap	0.579	0.605	0.644	0.645	0.565	0.501	0.656	0.652
Aug_KL	0.665	0.568	0.537	0.549	0.636	0.540	0.538	0.552
MaxRényi	0.702	0.726	0.709	0.743	0.647	0.682	0.728	0.738
<b>Ours</b> (Image_Sim, Gaussian Blur, Kernel Size 5)			0.881				0.878	
<b>Ours</b> (Image_Sim, Motion Blur Kernel Size 5)			0.860				0.856	
<b>Ours</b> (Image_Sim, JPEG Compression, Quality = 5)			0.682				0.681	

Table 2: TPR at 5% FPR of various baseline methods under Li et al. (2024b)’s pipeline and our proposed approach on VL-MIA/Flickr. The column 'img', 'inst', 'desp', and 'inst+desp' has the same meaning as the previous table.

Method	LLaVA-1.5-7B				LLaVA-1.5-13B			
	img	inst	desp	inst+desp	img	inst	desp	inst+desp
Perplexity	-	0.007	0.137	0.067	-	0.047	0.227	0.127
Min_20% Prob	-	0.007	0.127	0.003	-	0.067	0.163	0.053
ModRényi	-	0.003	0.113	0.113	-	0.060	0.203	0.147
Max_Prob_Gap	0.050	0.083	0.163	0.163	0.050	0.107	0.163	0.160
Aug_KL	0.080	0.073	0.060	0.043	0.133	0.070	0.050	0.060
MaxRényi	0.100	0.210	0.163	0.127	0.077	0.073	0.213	0.183
<b>Ours</b> (Image_Sim, Gaussian Blur, Kernel Size 5)			0.333				0.323	
<b>Ours</b> (Image_Sim, Motion Blur Kernel Size 5)			0.363				0.297	
<b>Ours</b> (Image_Sim, JPEG Compression, Quality = 5)			0.057				0.060	

Image Similarity-based attack, we fix the Kernel Size of the Gaussian blur and the Motion blur as 5. For JPEG compression, the image quality is set to 5 (lower values indicate stronger compression). For the Text Similarity-based attack, following Li et al. (2024b), we use “Describe this image concisely” (Li et al., 2024b) as the prompt and the max generation token amount is 32. For simplicity, we only use Gaussian blur for Text Similarity-based attack and the kernel size is set to 45.

## 5.1 White-Box MIA Performance

The results on LLaVA 1.5 series are shown in Table 1 and Table 2. Results on VL-MIA/Flickr 2K are in Appendix D. Note that our methods have different knowledge of the models compared to the baseline methods. We can obtain the image embeddings while they can obtain the output text’s logits. We can observe that similarity-based attacks using Gaussian Blur and Motion Blur can achieve an AUC higher than 0.8 for both LLaVA 1.5-7B and LLaVA-1.5-13B, which is much higher than all the

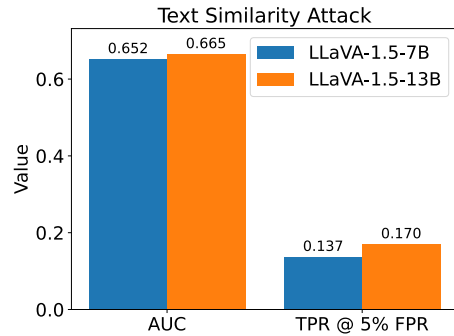


Figure 6: Text similarity-based membership inference attack on VL-MIA/Flickr. Image corruption method is Gaussian Blur and the kernel size is 45.

baselines. In comparison, the highest AUC among the baseline methods is 0.743 on LLaVA-1.5-7B and 0.738 on LLaVA-1.5-13B. Similar results can be found in Table 2, our methods largely outperform all the baselines in terms of TPR at 5% FPR where the best baseline performance is 0.210 on LLaVA-1.5-7B and 0.227 on LLaVA-1.5-13B.

It shows that using information from the visual side can better facilitate image MIAs compared

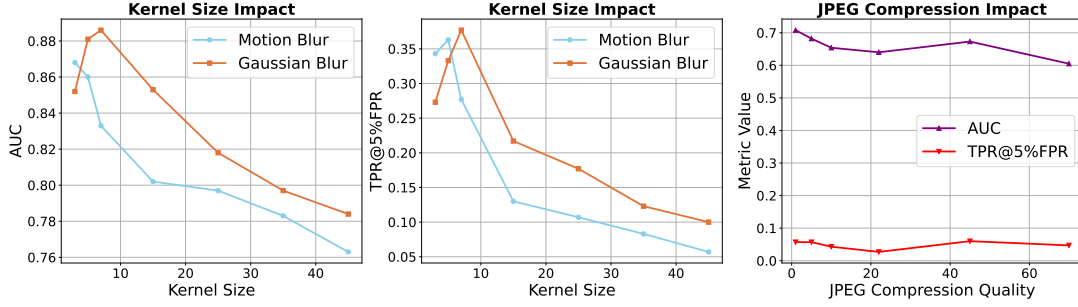


Figure 7: Analysis on Image Corruption Hyperparameters.

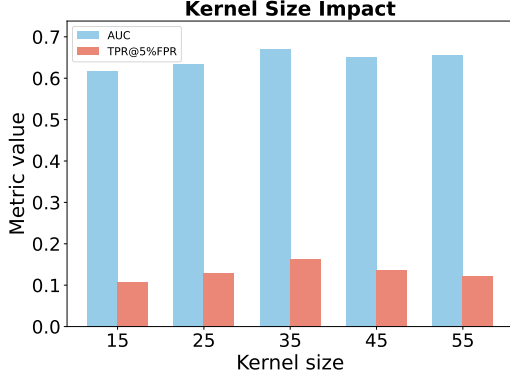


Figure 8: Kernel Size’s Impact on Text Similarity-based Attack.

with using information from different logit slices. The results also suggest that the image corruption method matters. For example, the performance using JPEG compression is worse than that using Gaussian Blur and Motion Blur.

## 5.2 Black-box MIA performance

The results of our attack method under the black-box setting, which is based on output texts’ embeddings, are shown in Figure 6. The results demonstrate the effectiveness of our method. For example, it achieves an AUC of 0.652 and a TPR@5%FPR of 0.137 on LLaVA-1.5-7B, which outperforms many baselines that require using output logits, even though our approach only queries the target model.

## 5.3 Hyperparameter Analysis

In this subsection, we conduct experiments to observe the impacts of hyperparameters. For the image similarity-based attack, we vary the kernel size for Gaussian Blur and Motion Blur using values of 3, 5, 7, 15, 25, 35, and 45. The image quality for JPEG compression is selected across 1, 5, 10, 20, 45, and 70. The selected model is LLaVA 1.5 7B. The results are shown in Figure 7. We can observe that smaller kernel sizes generally con-

tribute to better performance in terms of both AUC and TPR@5%FPR. Larger kernel sizes will bring stronger corruption. Therefore, for blur-based corruption methods, it suggests that it would be better to use a smaller corruption level for such methods. Although the performance drops a lot with very large kernel sizes, it still outperforms most baselines that rely on output logits. For the third sub-figure in Figure 7, we can see that a smaller JPEG quality (Stronger compression) generally leads to higher AUC.

For the text similarity-based attack, the kernel size for Gaussian Blur is varied across 15, 25, 35, 45 and 55. The results are shown in Figure 8. Unlike image similarity-based attacks, text similarity-based attacks generally perform better with larger kernel sizes. One possible reason is that if the kernel size is too small, small changes in the image embeddings lead to even smaller changes in the textual output. This makes the difference between member and non-member images less clear.

Table 3: Image MIA AUC and TPR at 5% FPR of our proposed approach on VL-MIA/Flickr. The embeddings are replaced with the ones obtained directly from the CLIP vision encoder without the alignment module.

Method	AUC		TPR@5%FPR	
	7B	13B	7B	13B
Ours (Gaussian Blur)	0.881	0.878	0.333	0.323
Ours (Gaussian Blur, CLIP)	0.885		0.413	
Ours (Motion Blur)	0.860	0.856	0.363	0.297
Ours (Motion Blur, CLIP)	0.858		0.393	
Ours (JPEG Compression)	0.682	0.681	0.057	0.060
Ours (JPEG Compression, CLIP)	0.705		0.103	

## 5.4 Extra Findings

We replace the embeddings obtained by the CLIP vision encoder and the alignment module with the embeddings directly from the CLIP vision encoder without passing them through the alignment module. The results are shown in Table 3. Interestingly, we find that using the embeddings directly from



the CLIP vision encoder can even have slightly better performance. However, the CLIP encoder is frozen during the training stage of LLaVA v 1.5. This suggests that the images were likely included in the CLIP model’s original training data. Our method’s high performance might also benefit from this. This suggests that we need some new benchmark datasets to better define the image MIA problem in the context of LVLMs.

## 6 Conclusion

In this paper, we design novel membership inference attack methods named ICIMIA against LVLMs under both white-box and black-box settings. Our approach is based on the observation that LVLMs exhibit varying sensitivity to image corruption for member and non-member images. We leverage this phenomenon by using the pair-wise similarity of the original version and its corrupted counterpart as the metric. Experimental results on existing datasets validate the effectiveness of our proposed methods.

## Limitations

We observed an interesting phenomenon: many non-member images generated by DALL-E (Ramesh et al., 2022) exhibit greater robustness to corruption compared to their original counterparts (the generated image is prompted to be similar to its original member image), regardless of whether the original image is a member or non-member. Therefore, our method does not work for such a dataset where each non-member image is generated by DALL-E based on the original member image. One example is the img\_dalle dataset Li et al. (2024b) where Blip (Li et al., 2023b) generates a caption for each member image and the caption is used by DALL-E to generate a non-member image for this image. We leave this as our future work.

## Ethical Considerations

Our work aims to find the images that are in the training data of large vision-language models. Our proposed method, ICIMIA, can help individuals know whether their sensitive data is used to train the model. All experiments are conducted on open-source models and publicly available datasets.

**AI Assistants In Writing.** In this paper, we only use AI assistants for grammar checking and sentence polishing.

## References

- Josh Achiam, Steven Adler, Sandhini Agarwal, Lama Ahmad, Ilge Akkaya, Florencia Leoni Aleman, Diogo Almeida, Janko Altschmidt, Sam Altman, Shyamal Anadkat, et al. 2023. Gpt-4 technical report. *arXiv preprint arXiv:2303.08774*.
- Jinze Bai, Shuai Bai, Yunfei Chu, Zeyu Cui, Kai Dang, Xiaodong Deng, Yang Fan, Wenbin Ge, Yu Han, Fei Huang, et al. 2023a. Qwen technical report. *arXiv preprint arXiv:2309.16609*.
- Jinze Bai, Shuai Bai, Shusheng Yang, Shijie Wang, Sinan Tan, Peng Wang, Junyang Lin, Chang Zhou, and Jingren Zhou. 2023b. Qwen-vl: A frontier large vision-language model with versatile abilities. *arXiv preprint arXiv:2308.12966*.
- Shuai Bai, Keqin Chen, Xuejing Liu, Jialin Wang, Wenbin Ge, Sibao Song, Kai Dang, Peng Wang, Shijie Wang, Jun Tang, et al. 2025. Qwen2. 5-vl technical report. *arXiv preprint arXiv:2502.13923*.
- G. Bratski. 2000. The OpenCV Library. *Dr. Dobbs’s Journal of Software Tools*.
- Davide Bucciarelli, Nicholas Moratelli, Marcella Cornia, Lorenzo Baraldi, and Rita Cucchiara. 2024. Personalizing multimodal large language models for image captioning: an experimental analysis. *arXiv preprint arXiv:2412.03665*.
- Minwoo Byeon, Beomhee Park, Haecheon Kim, Sungjun Lee, Woonhyuk Baek, and Saehoon Kim. 2022. Coyo-700m: Image-text pair dataset. <https://github.com/kakaobrain/coyo-dataset>.
- Nicholas Carlini, Steve Chien, Milad Nasr, Shuang Song, Andreas Terzis, and Florian Tramer. 2022a. Membership inference attacks from first principles. In *2022 IEEE symposium on security and privacy (SP)*, pages 1897–1914. IEEE.
- Nicholas Carlini, Daphne Ippolito, Matthew Jagielski, Katherine Lee, Florian Tramer, and Chiyuan Zhang. 2022b. Quantifying memorization across neural language models. In *The Eleventh International Conference on Learning Representations*.
- Nicholas Carlini, Chang Liu, Úlfar Erlingsson, Jernej Kos, and Dawn Song. 2019. The secret sharer: Evaluating and testing unintended memorization in neural networks. In *28th USENIX security symposium (USENIX security 19)*, pages 267–284.
- Nicholas Carlini, Florian Tramer, Eric Wallace, Matthew Jagielski, Ariel Herbert-Voss, Katherine Lee, Adam Roberts, Tom Brown, Dawn Song, Úlfar Erlingsson, et al. 2021. Extracting training data from large language models. In *30th USENIX security symposium (USENIX Security 21)*, pages 2633–2650.
- Soravit Changpinyo, Piyush Sharma, Nan Ding, and Radu Soricut. 2021. Conceptual 12m: Pushing web-scale image-text pre-training to recognize long-tail

- visual concepts. In *Proceedings of the IEEE/CVF conference on computer vision and pattern recognition*, pages 3558–3568.
- Jun Chen, Deyao Zhu, Xiaoqian Shen, Xiang Li, Zechu Liu, Pengchuan Zhang, Raghuraman Krishnamoorthi, Vikas Chandra, Yuniang Xiong, and Mohamed Elhoseiny. 2023. Minigpt-v2: large language model as a unified interface for vision-language multi-task learning. *arXiv preprint arXiv:2310.09478*.
- Zhe Chen, Weiyun Wang, Yue Cao, Yangzhou Liu, Zhangwei Gao, Erfei Cui, Jinguo Zhu, Shenglong Ye, Hao Tian, Zhaoyang Liu, et al. 2024a. Expanding performance boundaries of open-source multimodal models with model, data, and test-time scaling. *arXiv preprint arXiv:2412.05271*.
- Zhe Chen, Weiyun Wang, Hao Tian, Shenglong Ye, Zhangwei Gao, Erfei Cui, Wenwen Tong, Kongzhi Hu, Jiapeng Luo, Zheng Ma, et al. 2024b. How far are we to gpt-4v? closing the gap to commercial multimodal models with open-source suites. *arXiv preprint arXiv:2404.16821*.
- Zhe Chen, Jiannan Wu, Wenhai Wang, Weijie Su, Guo Chen, Sen Xing, Muyan Zhong, Qinglong Zhang, Xizhou Zhu, Lewei Lu, et al. 2024c. Internvl: Scaling up vision foundation models and aligning for generic visual-linguistic tasks. In *Proceedings of the IEEE/CVF Conference on Computer Vision and Pattern Recognition*, pages 24185–24198.
- Wei-Lin Chiang, Zhuohan Li, Zi Lin, Ying Sheng, Zhanghao Wu, Hao Zhang, Lianmin Zheng, Siyuan Zhuang, Yonghao Zhuang, Joseph E. Gonzalez, Ion Stoica, and Eric P. Xing. 2023. *Vicuna: An open-source chatbot impressing gpt-4 with 90%\* chatgpt quality*.
- Christopher A. Choquette-Choo, Florian Tramer, Nicholas Carlini, and Nicolas Papernot. 2021. Label-only membership inference attacks. In *Proceedings of the 38th International Conference on Machine Learning*, pages 1964–1974. PMLR.
- Hongyuan Dong, Jiawen Li, Bohong Wu, Jiacong Wang, Yuan Zhang, and Haoyuan Guo. 2024. Benchmarking and improving detail image caption. *arXiv preprint arXiv:2405.19092*.
- Kimi Team Angang Du, Bohong Yin, Bowei Xing, Bowen Qu, Bowen Wang, Cheng Chen, Chenlin Zhang, Chenzhuang Du, Chu Wei, Congcong Wang, Dehao Zhang, Dikang Du, Dongliang Wang, Enming Yuan, Enzhe Lu, Fang Li, Flood Sung, Guangda Wei, Guokun Lai, Han Zhu, Hao Ding, Hao-Xing Hu, Hao Yang, Hao Zhang, Haoning Wu, Haotian Yao, Haoyu Lu, Heng Wang, Hongcheng Gao, Huabin Zheng, Jiaming Li, Jianling Su, Jianzhou Wang, Jiaqi Deng, Jiezhong Qiu, Jin Xie, Jinhong Wang, Jingyuan Liu, Junjie Yan, Kun Ouyang, Liang Chen, Lin Sui, Long Yu, Mengfan Dong, Meng Dong, Nuo Xu, Peng Cheng, Qizheng Gu, Runjie Zhou, Shaowei Liu, Si-han Cao, Tao Yu, Tianhui Song, Tongtong Bai, Wei Song, Weiran He, Weixiao Huang, Weixin Xu, Xiaofeng Yuan, Xingcheng Yao, Xingzhe Wu, Xinxing Zu, Xinyu Zhou, Xinyuan Wang, Y. Charles, Yan-Qing Zhong, Yang Li, Yan-Ni Hu, Yanru Chen, Ye-Jia Wang, Yibo Liu, Yibo Miao, Yidao Qin, Yimin Chen, Yiping Bao, Yiqin Wang, Yongsheng Kang, Yuan-Qing Liu, Yulun Du, Yuxin Wu, Yuzhi Wang, Yuzi Yan, Zaida Zhou, Zhaowei Li, Zhejun Jiang, Zheng Zhang, Zhilin Yang, Zhiqi Huang, Zihao Huang, Zijia Zhao, and Ziwei Chen. 2025. Kimi-vl technical report. *arXiv preprint arXiv:2504.07491*.
- Michael Duan, Anshuman Suri, Niloofar Mireshghallah, Sewon Min, Weijia Shi, Luke Zettlemoyer, Yulia Tsvetkov, Yejin Choi, David Evans, and Hannaneh Hajishirzi. 2024. Do membership inference attacks work on large language models? *arXiv preprint arXiv:2402.07841*.
- Chaoyou Fu, Yi-Fan Zhang, Shukang Yin, Bo Li, Xinyu Fang, Sirui Zhao, Haodong Duan, Xing Sun, Ziwei Liu, Liang Wang, et al. 2024. Mme-survey: A comprehensive survey on evaluation of multimodal llms. *arXiv preprint arXiv:2411.15296*.
- Aaron Grattafiori, Abhimanyu Dubey, Abhinav Jauhri, Abhinav Pandey, Abhishek Kadian, Ahmad Al-Dahle, Aiesha Letman, Akhil Mathur, Alan Schelten, Alex Vaughan, et al. 2024. The llama 3 herd of models. *arXiv preprint arXiv:2407.21783*.
- Hongsheng Hu, Zoran Salcic, Lichao Sun, Gillian Dobbie, Philip S. Yu, and Xuyun Zhang. 2022a. *Membership inference attacks on machine learning: A survey*. *ACM Comput. Surv.*, 54(11s).
- Pingyi Hu, Zihan Wang, Ruoxi Sun, Hu Wang, and Minhui Xue. 2022b. M4 i: Multi-modal models membership inference. *Advances in Neural Information Processing Systems*, 35:1867–1882.
- Yuke Hu, Zheng Li, Zhihao Liu, Yang Zhang, Zhan Qin, Kui Ren, and Chun Chen. 2025. Membership inference attacks against vision-language models. *arXiv preprint arXiv:2501.18624*.
- Albert Qiaochu Jiang, Alexandre Sablayrolles, Arthur Mensch, Chris Bamford, Devendra Singh Chaplot, Diego de Las Casas, Florian Bressand, Gianna Lengyel, Guillaume Lample, Lucile Saulnier, L’elio Renard Lavaud, Marie-Anne Lachaux, Pierre Stock, Teven Le Scao, Thibaut Lavril, Thomas Wang, Timothée Lacroix, and William El Sayed. 2023. Mistral 7b. *arXiv preprint arXiv:2310.06825*.
- Myeongseob Ko, Ming Jin, Chenguang Wang, and Ruoxi Jia. 2023. Practical membership inference attacks against large-scale multi-modal models: A pilot study. In *Proceedings of the IEEE/CVF International Conference on Computer Vision*, pages 4871–4881.
- Klas Leino and Matt Fredrikson. 2020. Stolen memories: Leveraging model memorization for calibrated {White-Box} membership inference. In *29th USENIX security symposium (USENIX Security 20)*, pages 1605–1622.

- Bohao Li, Yuying Ge, Yi Chen, Yixiao Ge, Ruimao Zhang, and Ying Shan. 2024a. Seed-bench-2-plus: Benchmarking multimodal large language models with text-rich visual comprehension. *arXiv preprint arXiv:2404.16790*.
- Chunyuan Li, Cliff Wong, Sheng Zhang, Naoto Usuyama, Haotian Liu, Jianwei Yang, Tristan Naumann, Hoifung Poon, and Jianfeng Gao. 2023a. Llava-med: Training a large language-and-vision assistant for biomedicine in one day. *Advances in Neural Information Processing Systems*, 36:28541–28564.
- Jiacheng Li, Ninghui Li, and Bruno Ribeiro. 2021. Membership inference attacks and defenses in classification models. In *Proceedings of the Eleventh ACM Conference on Data and Application Security and Privacy*, pages 5–16.
- Junnan Li, Dongxu Li, Silvio Savarese, and Steven Hoi. 2023b. Blip-2: Bootstrapping language-image pre-training with frozen image encoders and large language models. In *International conference on machine learning*, pages 19730–19742. PMLR.
- Zhan Li, Yongtao Wu, Yihang Chen, Francesco Tonin, Elías Abad-Rocamora, and Volkan Cevher. 2024b. [Membership inference attacks against large vision-language models](#). In *Annual Conference on Neural Information Processing Systems, NeurIPS*.
- Zhang Li, Biao Yang, Qiang Liu, Zhiyin Ma, Shuo Zhang, Jingxu Yang, Yabo Sun, Yuliang Liu, and Xiang Bai. 2024c. Monkey: Image resolution and text label are important things for large multi-modal models. In *proceedings of the IEEE/CVF conference on computer vision and pattern recognition*.
- Tsung-Yi Lin, Michael Maire, Serge Belongie, James Hays, Pietro Perona, Deva Ramanan, Piotr Dollár, and C Lawrence Zitnick. 2014. Microsoft coco: Common objects in context. In *Computer vision—ECCV 2014: 13th European conference, zurich, Switzerland, September 6–12, 2014, proceedings, part v 13*, pages 740–755. Springer.
- Haotian Liu, Chunyuan Li, Yuheng Li, and Yong Jae Lee. 2024a. Improved baselines with visual instruction tuning. In *Proceedings of the IEEE/CVF Conference on Computer Vision and Pattern Recognition*, pages 26296–26306.
- Haotian Liu, Chunyuan Li, Yuheng Li, Bo Li, Yuanhan Zhang, Sheng Shen, and Yong Jae Lee. 2024b. [Llava-next: Improved reasoning, ocr, and world knowledge](#).
- Haotian Liu, Chunyuan Li, Qingyang Wu, and Yong Jae Lee. 2024c. Visual instruction tuning. *Advances in neural information processing systems*, 36.
- Hongbin Liu, Jinyuan Jia, Wenjie Qu, and Neil Zhenqiang Gong. 2021. Encodermi: Membership inference against pre-trained encoders in contrastive learning. In *Proceedings of the 2021 ACM SIGSAC Conference on Computer and Communications Security*, pages 2081–2095.
- Justus Mattern, Fatemehsadat Miresghallah, Zhijing Jin, Bernhard Schölkopf, Mrinmaya Sachan, and Taylor Berg-Kirkpatrick. 2023. Membership inference attacks against language models via neighbourhood comparison. *arXiv preprint arXiv:2305.18462*.
- Fatemehsadat Miresghallah, Archit Uniyal, Tianhao Wang, David K Evans, and Taylor Berg-Kirkpatrick. 2022. An empirical analysis of memorization in fine-tuned autoregressive language models. In *Proceedings of the 2022 Conference on Empirical Methods in Natural Language Processing*, pages 1816–1826.
- Milad Nasr, Reza Shokri, and Amir Houmansadr. 2019. Comprehensive privacy analysis of deep learning: Passive and active white-box inference attacks against centralized and federated learning. In *2019 IEEE symposium on security and privacy (SP)*, pages 739–753. IEEE.
- Edwin G. Ng, Bo Pang, Piyush Sharma, and Radu Soricut. 2020. Understanding guided image captioning performance across domains. *arXiv preprint arXiv:2012.02339*.
- Yonatan Oren, Nicole Meister, Niladri Chatterji, Faisal Ladhak, and Tatsunori B Hashimoto. 2023. Proving test set contamination in black box language models. *arXiv preprint arXiv:2310.17623*.
- Guilherme Penedo, Quentin Malartic, Daniel Hesslow, Ruxandra Cojocaru, Alessandro Cappelli, Hamza Alobeidli, Baptiste Pannier, Ebtesam Almazrouei, and Julien Launay. 2023. The refinedweb dataset for falcon llm: outperforming curated corpora with web data, and web data only. *arXiv preprint arXiv:2306.01116*.
- Alec Radford, Jong Wook Kim, Chris Hallacy, Aditya Ramesh, Gabriel Goh, Sandhini Agarwal, Girish Sastry, Amanda Askell, Pamela Mishkin, Jack Clark, et al. 2021. Learning transferable visual models from natural language supervision. In *International conference on machine learning*, pages 8748–8763. PMLR.
- Aditya Ramesh, Prafulla Dhariwal, Alex Nichol, Casey Chu, and Mark Chen. 2022. Hierarchical text-conditional image generation with clip latents. *arXiv preprint arXiv:2204.06125*, 1(2):3.
- Jie Ren, Kangrui Chen, Chen Chen, Vikash Sehwal, Yue Xing, Jiliang Tang, and Lingjuan Lyu. 2024. Self-comparison for dataset-level membership inference in large (vision-) language models. *arXiv preprint arXiv:2410.13088*.
- Alfréd Rényi. 1961. On measures of entropy and information. In *Proceedings of the fourth Berkeley symposium on mathematical statistics and probability, volume 1: contributions to the theory of statistics*, volume 4, pages 547–562. University of California Press.
- Shahbaz Rezaei and Xin Liu. 2021. On the difficulty of membership inference attacks. In *Proceedings of the IEEE/CVF Conference on Computer Vision and Pattern Recognition*, pages 7892–7900.



- Alexandre Sablayrolles, Matthijs Douze, Cordelia Schmid, Yann Ollivier, and Hervé Jégou. 2019. White-box vs black-box: Bayes optimal strategies for membership inference. In *International Conference on Machine Learning*, pages 5558–5567. PMLR.
- Ahmed Salem, Yang Zhang, Mathias Humbert, Pascal Berrang, Mario Fritz, and Michael Backes. 2018. MI-leaks: Model and data independent membership inference attacks and defenses on machine learning models. *arXiv preprint arXiv:1806.01246*.
- Weijia Shi, Anirudh Ajith, Mengzhou Xia, Yangsibo Huang, Daogao Liu, Terra Blevins, Danqi Chen, and Luke Zettlemoyer. 2024. [Detecting pretraining data from large language models](#). In *The Twelfth International Conference on Learning Representations, ICLR*. OpenReview.net.
- Reza Shokri, Marco Stronati, Congzheng Song, and Vitaly Shmatikov. 2017. Membership inference attacks against machine learning models. In *2017 IEEE symposium on security and privacy (SP)*, pages 3–18. IEEE.
- Congzheng Song, Thomas Ristenpart, and Vitaly Shmatikov. 2017. Machine learning models that remember too much. In *Proceedings of the 2017 ACM SIGSAC Conference on computer and communications security*, pages 587–601.
- InternLM Team. 2023. Internlm: A multilingual language model with progressively enhanced capabilities. <https://github.com/InternLM/InternLM-techreport>.
- Shengbang Tong, Ellis Brown, Penghao Wu, Sanghyun Woo, Manoj Middepogu, Sai Charitha Akula, Jihan Yang, Shusheng Yang, Adithya Iyer, Xichen Pan, et al. 2024. Cambrian-1: A fully open, vision-centric exploration of multimodal llms. *arXiv preprint arXiv:2406.16860*.
- Hugo Touvron, Thibaut Lavril, Gautier Izacard, Xavier Martinet, Marie-Anne Lachaux, Timothée Lacroix, Baptiste Rozière, Naman Goyal, Eric Hambro, Faisal Azhar, et al. 2023a. Llama: Open and efficient foundation language models. *arXiv preprint arXiv:2302.13971*.
- Hugo Touvron, Louis Martin, Kevin Stone, Peter Albert, Amjad Almahairi, Yasmine Babaei, Nikolay Bashlykov, Soumya Batra, Prajjwal Bhargava, Shruti Bhosale, et al. 2023b. Llama 2: Open foundation and fine-tuned chat models. *arXiv preprint arXiv:2307.09288*.
- Fali Wang, Zhiwei Zhang, Xianren Zhang, Zongyu Wu, Tzuhaio Mo, Qiuhaio Lu, Wanqing Wang, Rui Li, Junjie Xu, Xianfeng Tang, et al. 2024. A comprehensive survey of small language models in the era of large language models: Techniques, enhancements, applications, collaboration with llms, and trustworthiness. *arXiv preprint arXiv:2411.03350*.
- Zongyu Wu, Yuwei Niu, Hongcheng Gao, Minhua Lin, Zhiwei Zhang, Zhifang Zhang, Qi Shi, Yilong Wang, Sike Fu, Junjie Xu, et al. 2025. Lanp: Rethinking the impact of language priors in large vision-language models. *arXiv preprint arXiv:2502.12359*.
- Junjie Xu, Zongyu Wu, Minhua Lin, Xiang Zhang, and Suhang Wang. 2024. Llm and gnn are complementary: Distilling llm for multimodal graph learning. *arXiv preprint arXiv:2406.01032*.
- An Yang, Anfeng Li, Baosong Yang, Beichen Zhang, Binyuan Hui, Bo Zheng, Bowen Yu, Chang Gao, Chengen Huang, Chenxu Lv, et al. 2025. Qwen3 technical report. *arXiv preprint arXiv:2505.09388*.
- An Yang, Baosong Yang, Binyuan Hui, Bo Zheng, Bowen Yu, Chang Zhou, Chengpeng Li, Chengyuan Li, Dayiheng Liu, Fei Huang, Guanting Dong, Haoran Wei, Huan Lin, Jialong Tang, Jialin Wang, Jian Yang, Jianhong Tu, Jianwei Zhang, Jianxin Ma, Jin Xu, Jingren Zhou, Jinze Bai, Jinzheng He, Junyang Lin, Kai Dang, Keming Lu, Ke-Yang Chen, Kexin Yang, Mei Li, Min Xue, Na Ni, Pei Zhang, Peng Wang, Ru Peng, Rui Men, Ruize Gao, Runji Lin, Shijie Wang, Shuai Bai, Sinan Tan, Tianhang Zhu, Tianhao Li, Tianyu Liu, Wenbin Ge, Xiaodong Deng, Xiaohuan Zhou, Xingzhang Ren, Xinyu Zhang, Xipin Wei, Xuancheng Ren, Yang Fan, Yang Yao, Yichang Zhang, Yunyang Wan, Yunfei Chu, Zeyu Cui, Zhenru Zhang, and Zhi-Wei Fan. 2024. Qwen2 technical report. *arXiv preprint arXiv:2407.10671*.
- Alex Young, Bei Chen, Chao Li, Chengen Huang, Ge Zhang, Guanwei Zhang, Guoyin Wang, Heng Li, Jiangcheng Zhu, Jianqun Chen, et al. 2024. Yi: Open foundation models by 01. ai. *arXiv preprint arXiv:2403.04652*.
- Xiang Yue, Yuansheng Ni, Kai Zhang, Tianyu Zheng, Ruoqi Liu, Ge Zhang, Samuel Stevens, Dongfu Jiang, Weiming Ren, Yuxuan Sun, Cong Wei, Botao Yu, Ruibin Yuan, Renliang Sun, Ming Yin, Boyuan Zheng, Zhenzhu Yang, Yibo Liu, Wenhao Huang, Huan Sun, Yu Su, and Wenhao Chen. 2024. Mmmu: A massive multi-discipline multimodal understanding and reasoning benchmark for expert agi. In *Proceedings of the IEEE/CVF Conference on Computer Vision and Pattern Recognition*.
- Jingyang Zhang, Jingwei Sun, Eric Yeats, Yang Ouyang, Martin Kuo, Jianyi Zhang, Hao Frank Yang, and Hai Li. 2024. Min-k%++: Improved baseline for detecting pre-training data from large language models. *arXiv preprint arXiv:2404.02936*.
- Renrui Zhang, Jiaming Han, Chris Liu, Peng Gao, Aojun Zhou, Xiangfei Hu, Shilin Yan, Pan Lu, Hongsheng Li, and Yu Qiao. 2023. Llama-adapter: Efficient fine-tuning of language models with zero-init attention. *arXiv preprint arXiv:2303.16199*.
- Wayne Xin Zhao, Kun Zhou, Junyi Li, Tianyi Tang, Xiaolei Wang, Yupeng Hou, Yingqian Min, Beichen Zhang, Junjie Zhang, Zican Dong, et al. 2023. A



survey of large language models. *arXiv preprint arXiv:2303.18223*, 1(2).

Deyao Zhu, Jun Chen, Xiaoqian Shen, Xiang Li, and Mohamed Elhoseiny. 2023. Minigpt-4: Enhancing vision-language understanding with advanced large language models. *arXiv preprint arXiv:2304.10592*.

Jinguo Zhu, Weiyun Wang, Zhe Chen, Zhaoyang Liu, Shenglong Ye, Lixin Gu, Hao Tian, Yuchen Duan, Weijie Su, Jie Shao, et al. 2025. Internv13: Exploring advanced training and test-time recipes for open-source multimodal models. *arXiv preprint arXiv:2504.10479*.

## A Details of Datasets

Many models, such as LLaVA 1.5 and Minigpt 4 (Zhu et al., 2023), use MS COCO (Lin et al., 2014) to train the models. Therefore, Li et al. (2024b) use part of the images in MS COCO as the member images. For non-member data, Li et al. (2024b) select images uploaded to Flickr<sup>2</sup> after those models’ release date. The datasets are licensed under the Creative Commons Attribution 4.0 International License. The dataset statistics are summarized in Table 4.

## B Examples of Different Corruptions

In this section, we show some examples of different types of corruption. The examples are shown in Figure 9. The original image is from the VL-MIA/Flickr (Li et al., 2024b) dataset and is sourced from: <https://www.flickr.com/photos/9750464@N02/53573626031>

## C Used Metrics

We provide details about two used metrics here:

- **AUC:** Area Under the Curve (AUC) is the value of the area beneath the ROC curve. It is a widely used metric to evaluate the classification model’s performance under all possible classification thresholds (Li et al., 2024b).
- **TPR at 5% FPR:** True Positive Rate at 5% False Positive Rate (TPR at 5% FPR) is another widely used metric to evaluate the performance of a classification model (Li et al., 2024b; Carlini et al., 2022a). It reflects the value of the True Positive Rate when the False Positive Rate is 5%.

## D Additional Results

We conduct experiments on VL-MIA/Flickr-2K. The image similarity-based MIA results are shown in Table 5 and Table 6. We can have similar observations as in Table 1 and Table 2. The experimental results on VL-MIA/Flickr-2K also validate the effectiveness of our proposed methods.

## E Potential Risks

Although our proposed ICIMIA is designed to protect data integrity, malicious users can use ICIMIA to infer whether an image is used to train a certain

LVLM and then get some private information. For example, if the attacker knows that one person’s medical image is used to train an LVLM for a certain disease, the attacker can get the information that this person is likely to have this disease.

---

<sup>2</sup><https://www.flickr.com/>

Table 4: Dataset statistics. The datasets are constructed by (Li et al., 2024b)

Name	Member Data	Non-member Data	#Memembr Data	#Non-member Data
VL-MIA/Flickr	MS COCO	Flickr	300	300
VL-MIA/Flickr 2K	MS COCO	Flickr	1000	1000



Figure 9: Examples of different corruption methods.

Table 5: Image MIA AUC performance of our proposed approach on VL-MIA/Flickr 2K.

Method	LLaVA-1.5-7B	LLaVA-1.5-13B
<b>Ours</b> (Image_Sim, Gaussian Blur, Kernel Size 5)	0.854	0.850
<b>Ours</b> (Image_Sim, Motion Blur, Kernel Size 5)	0.842	0.837
<b>Ours</b> (Image_Sim, JPEG Compression, Quality = 5)	0.629	0.635

Table 6: Image MIA **TPR at 5% FPR** performance of our proposed approach on VL-MIA/Flickr 2K.

Method	LLaVA-1.5-7B	LLaVA-1.5-13B
<b>Ours</b> (Image_Sim, Gaussian Blur, Kernel Size 5)	0.349	0.337
<b>Ours</b> (Image_Sim, Motion Blur, Kernel Size 5)	0.372	0.352
<b>Ours</b> (Image_Sim, JPEG Compression, Quality = 5)	0.088	0.080